

# Evaluation of the Reconfiguration Effects of Planetary Rovers on their Lateral Traversing of Sandy Slopes

Hiroaki Inotsume, Masataku Sutoh, Kenji Nagaoka, Keiji Nagatani and Kazuya Yoshida

**Abstract**—Rovers that are used to explore craters on the Moon or Mars require the mobility to negotiate sandy slopes, on which slippage can easily occur. Such slippage can be reduced by actively readjusting the attitude of the rovers. By changing attitude, rovers can modify the position of their center of gravity and the wheel-soil contact angle. In this study, we discuss the effects of attitude changes on downhill sideslip based on the slope failure mechanism and experiments on reconfiguring the rover attitude and wheel angles. We conducted slope-traversing experiments using a wheeled rover under various roll angles and wheel angles. The experimental results show that the contact angle between wheels and slopes has a dominant influence on sideslip when compared with that of readjusting the rover's center of gravity.

## I. INTRODUCTION

Space agencies worldwide are planning missions to explore the surfaces of the Moon and Mars by using mobile robots or rovers. The several surface exploration missions to date have mainly succeeded because these explorations have been limited to benign terrains. Consequently, rovers in future missions are expected to probe more challenging surface geography, such as the rims or insides of craters. However, since the surfaces of the Moon and Mars are covered with fine-grained sand, when rovers traverse the slopes of their craters, both longitudinal and lateral slippage can easily occur, thereby jeopardizing the exploration. Because of longitudinal slip, the wheels can sink into loose soil while slipping, and in the worst-case scenario, the rover may not be able to move. Because of sideslip, the rover may deviate from the planned path or collide with unexpected obstacles.

To avoid these situations, it is essential to factor in the wheel-soil interaction mechanism at the design and development stage of exploration rovers. The field of terramechanics, which has been developed and organized by Bekker and Wong [1], [2], includes the study of such mechanisms. Based on terramechanics, several methods to estimate longitudinal mobility have been suggested (for example, [3]-[5]). Further, many studies have examined locomotion mechanisms that can generate high traction on loose soil [6]-[8]. However, few researchers thus far have considered the phenomenon of sideslip for planetary rovers. Helmick et al. [9] suggested a slip-compensated path-following method, in which a rover's longitudinal and lateral slippage is detected by visual odometry. Ishigami et al. [10] developed a path-following control method based on terramechanical models considering sideslip.

On the other hand, rovers that can actively modify their alignment or configuration to adapt to rough environments have attracted considerable attention. Such rovers are called "reconfigurable robots" [12], and several studies have examined their potential to negotiate challenging terrains [11]-[16]. Thus far, studies on reconfigurable rovers have primarily focused on the improvement of their traction or rollover stability on rough terrains [11]-[14]. Moreover, a few researchers have studied the effect of reconfiguration on slippage [15], [16]. Ishigami et al. [15] analyzed the effect of the position of the rover's center of gravity on vehicle gradeability over loose soil slopes. Wettergreen et al. [16] experimentally showed that downhill sideslip can be reduced by tilting a rover along the uphill direction when the rover is traversing sandy slopes. However, the relationship between such attitude change and downhill sideslip has not been sufficiently analyzed. If the forces between wheels and soil are estimated, sideslip can be minimized on arbitrary slopes by optimizing the configuration of the rover.

Our objective is to suggest methods to reduce sideslip over loose soil slopes. In this study, we evaluated the effects of the changes in the attitude of a rover on its sideslip. The attitude change of the rover depends on two factors - the position of the rover's center of gravity (COG) and the contact angle between the wheels and the soil. We assumed that downhill slip on loose soil occurs primarily due to slope failure, and we examined the effects of the abovementioned two factors based on slope failure. In order to validate this assumption and evaluate the effects of these factors on sideslip, we conducted slope-traversing experiments using a four-wheeled rover under various roll angles and wheel angles. Subsequently, we evaluated the influence of vehicle attitude change based on the experimental results.

## II. INFLUENCE OF ROVER ATTITUDE CHANGE ON SIDESLIP

### A. Evaluation indicator of mobility on loose soil slopes

Fig. 1 shows a rover laterally traversing a sandy slope with an angle of  $\alpha$  degrees. In this context, we define the slope coordinate system,  $\Sigma_s$ , as follows:  $x$  denotes the desired traversing direction,  $y$  denotes the uphill direction, and  $z$  denotes the vertically upward direction on the slope, thereby forming a right-handed coordinate system. When the rover drives over soil and displaces the soil, the forces act on the wheels, called the drawbar pull, side force, and vertical force along  $x$ ,  $y$  and  $z$  directions, respectively. In addition, gravitational forces act on the wheel along the negative  $y$  and

The authors are with the Department of Aerospace Engineering, Tohoku University, Aoba 6-6-01, Sendai, 980-8579, Japan, {inotsume, sutoh, nagaoka, keiji, yoshida}@astro.mech.tohoku.ac.jp

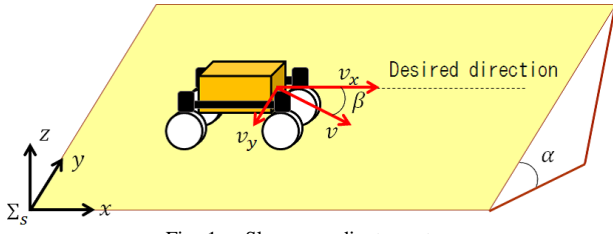


Fig. 1. Slope coordinate system

$z$  directions. As a result, the rover has a traveling velocity,  $v$ , defined by  $v = [v_x, v_y, v_z]^T$ .

One of the assessment criteria of the rover's mobility on sandy slopes is its slip angle. Here, the slip angle  $\beta$  is defined as the angle between the desired directional velocity  $v_x$  and lateral velocity  $v_y$  as follows [17]:

$$\beta = \tan^{-1} \left( \frac{v_y}{v_x} \right). \quad (1)$$

$\beta$  represents the degree of sideslip. According to this definition, the lesser the value of  $\beta$ , the greater is the rover's mobility.

### B. Sideslip due to slope failure

One reason of sideslip on loose sand slopes is the failure of the slopes. This section describes sideslip due to slope failure based on the stresses acting on the soil.

Fig. 2 depicts a smooth and uniform slope inclined at  $\alpha$  degrees, and a soil element with unit length, unit width, and depth  $h$ . Here,  $\rho$  denotes the density of the soil element. Consequently, the vertical pressure acting at the bottom of the element is given by

$$p_s = \rho g h \cos \alpha. \quad (2)$$

Therefore, the normal stress  $\sigma_s$  and shear stress  $\tau_s$  acting at the bottom due to the soil's weight are calculated as

$$\sigma_s = p_s \cos \alpha = \rho g h \cos^2 \alpha, \quad (3)$$

$$\tau_s = p_s \sin \alpha = \rho g h \cos \alpha \sin \alpha. \quad (4)$$

On the other hand, the resistant shear stress  $\tau_r$  acts at the bottom along a direction inverse to that of the shear stress  $\tau_s$ . This stress  $\tau_r$  reaches soil-specific limitation values when soil failure occurs, and these values are defined as the shear strength values. According to Mohr-Coulomb's failure criterion, the shear strength  $s$  is given as follows:

$$s = \tau_{r_{max}} = c + \sigma_s \tan \phi, \quad (5)$$

where  $c$  and  $\phi$  denote the soil-specific parameters of cohesion and internal friction angle, respectively. By substituting (3) into (5), we obtain shear strength on the slope as follows [18]:

$$s = c + \rho g h \cos^2 \alpha \tan \phi \quad (6)$$

Fig. 3 shows the relationship between the slope angle  $\alpha$ , shear strength  $s$ , and shear stress  $\tau$  in the case of Toyoura standard sand (JIS R 5201, dry sand,  $c = 0$  [Pa],  $\phi = 38$  [deg],  $\rho = 1.49 \times 10^3$  [kg/m<sup>3</sup>]). As observed in the figure,

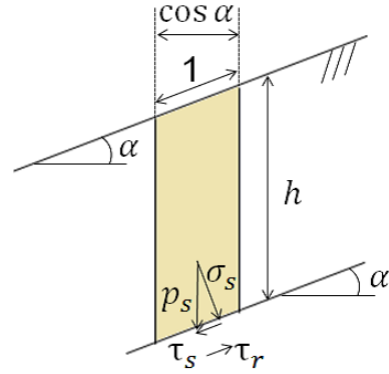


Fig. 2. Soil stress within a slope

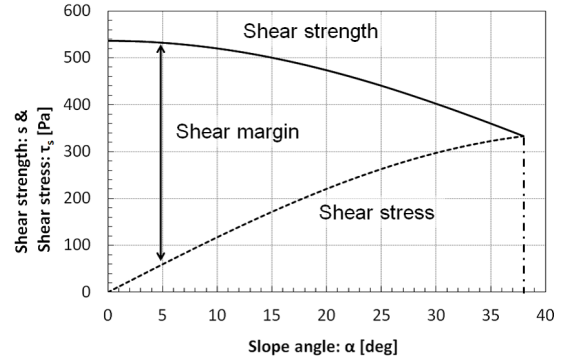


Fig. 3. Shear strength and shear stress vs. slope angle ( $h = 0.05$  [m]) for Toyoura sand

an increase in slope angle leads to increase in shear stress  $\tau_s$  and decrease in shear strength  $s$ . When the slope angle becomes larger than the internal friction angle  $\phi$  ( $38^\circ$ ),  $\tau_s$  becomes larger than  $s$ , and the soil element collapses along the downhill direction due to its own weight.

We applied the above theory for developing a sideslip mechanism on a slope. We define the difference between shear strength and shear stress ( $s - \tau_s$ ) as the shear margin. When a wheel traverses a slope, the wheel generates a stress on the soil along the downhill direction. If this stress is lesser than the shear margin of the slope, the slope is stable and sideslip due to slope failure does not occur. In contrast, when the stress is greater than the shear margin, soil failure will occur along a section of the soil and the wheel will undergo sideslip.

### C. Effects of rover attitude change

We assumed that the effect of the rover's attitude change on sideslip is composed of two key factors - the shift in the position of the rover's COG and the change in the wheel-soil contact angle.

1) *Effect of shift in the center of gravity:* Fig. 4 illustrates a four-wheeled rover traversing along a slope of  $\alpha$  degrees. The COG of the rover is located at a height  $L_h$  in the vertical direction of the slope and at distance  $L_u$  and  $L_d$  away from the uphill and downhill wheels, respectively, along its lateral direction. We assume that soil over the slope is uniform and the rover is traversing under static state. Consequently,

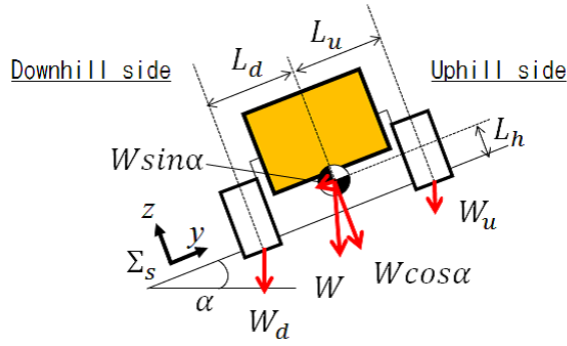


Fig. 4. Static rover model on a slope

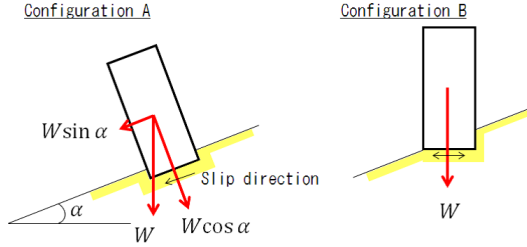


Fig. 5. Direction of slippage and gravity of a wheel

the forces acting on the uphill and downhill wheels are geometrically calculated as follows:

$$\text{Uphill side : } W_u = \frac{W(L_d \cos \alpha - L_h \sin \alpha)}{2(L_u + L_d) \cos \alpha}, \quad (7)$$

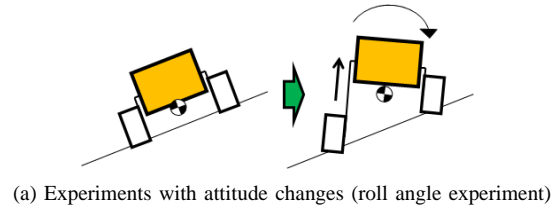
$$\text{Downhill side : } W_d = \frac{W(L_u \cos \alpha + L_h \sin \alpha)}{2(L_u + L_d) \cos \alpha}, \quad (8)$$

where  $W$  denotes the weight of the rover.

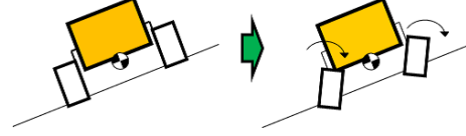
If  $L_u$  equals  $L_d$ , forces acting on the downhill wheels will be larger than those on the uphill wheels. In addition, when the loads on the wheels increase, the forces bulldozing the soil along the downhill direction also correspondingly increase. As described in Section II-B, when the soil is no longer capable of sustaining the bulldozing forces, it collapses, and the rover's wheels sideslip along the downhill direction. Based on this assumption, the sideslip can be reduced by shifting the COG upward along the slope so that the load on the downhill wheel does not cause the soil to collapse.

2) *Effect of the changing the wheel contact angle:* Fig. 5 depicts two types of wheel-soil contact conditions. Here, we assume that sideslip occurs along the bottom surface of the wheel. Then, if the wheel vertically contacts with the slope (configuration A in Fig. 5), gravitational force acting along the slip direction,  $W \sin \alpha$ , becomes large. Consequently, large stress will act on the soil around the wheel and sideslip will become significant.

On the other hand, the gravitational force along the wheel slip direction is reduced when the wheel is tilted along the uphill direction. Such directional force will be zero when the wheel horizontally contacts with the slope (configuration B



(a) Experiments with attitude changes (roll angle experiment)



(b) Experiments with wheel angle changes (wheel angle experiment)

Fig. 6. Comparison of the concepts of the two slope-traversing experiments

in Fig. 5). Furthermore, according to (6), the shear strength  $s$  of the soil is proportional to the depth of the soil element  $h$ . Therefore, when a wheel tilts toward uphill, the wheel tries to bulldoze the deeper area of soil which has greater shear strength. These effects follow that the occurrence of soil failure and the consequent downhill sideslip of the wheel are significantly reduced.

### III. SLOPE-TRAVERSING EXPERIMENTS

As mentioned above, a rover can traverse sandy slopes under the minimum amount of sideslip by optimizing its COG position and wheel-soil contact angle, thereby reducing the probability of slope failure.

In this study, to evaluate the effects of attitude change, i.e., shifting the rover's COG and changing the wheel-soil contact angle, we conducted two different slope-traversing experiments using a four-wheeled rover test bed. We first performed the experiment changing the attitude of the test bed as shown in Fig. 6(a). Next, experiment was conducted by varying the wheel angle of the test bed as shown in Fig. 6(b).

In this section, we describe the two types of experiments and their results. Then, we evaluate the effect of the rover's attitude changes on its sideslip.

#### A. Experiments with rover attitude changes

First, we conducted slope-traversing experiments under various roll angles.

TABLE I  
SPECIFICATIONS OF THE ROVER TEST BED FOR THE ROLL ANGLE  
EXPERIMENT (NOMINAL CONFIGURATION)

|                        |                              |
|------------------------|------------------------------|
| Size [mm]              | L800 × W650 × H400           |
| Mass [kg]              | 23.8                         |
| Wheel size [mm]        | φ200 × W100                  |
| Tread [mm]             | 550                          |
| Wheel base [mm]        | 600                          |
| Center of gravity [mm] | $L_d = L_u = 275, L_h = 187$ |

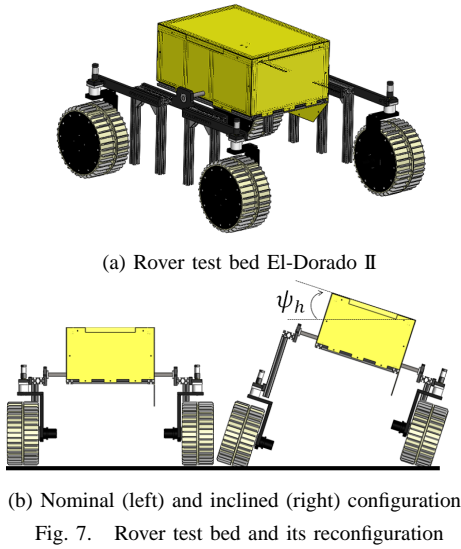


Fig. 7. Rover test bed and its reconfiguration

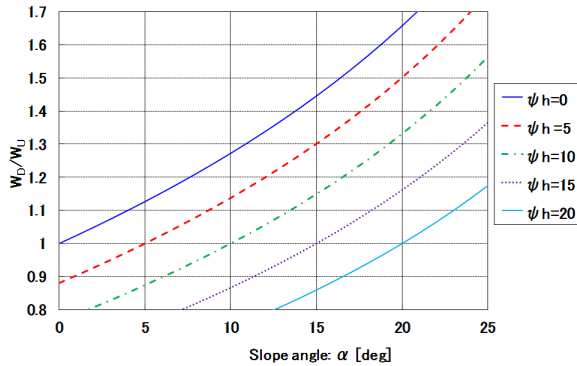


Fig. 8. Slope angle vs. ratio of wheel loads for various roll angles  $\psi_h$

1) *Experimental rover test bed*: We used a four-wheeled rover called El-Dorado II (illustrated in Fig. 7), as the test bed. The specifications of this rover are listed in Table I. The rover's left and right wheels are connected to each other by a rocker-link mechanism, and each wheel is equipped with grousers of 10 [mm] length on its surface at intervals of 10 [deg]. Furthermore, the attitude of the rover can be changed by manually sliding the wheel-attached part.

Here, we define the roll angle of the rover on a horizontal plane,  $\psi_h$ , as shown in Fig. 7 (b). We geometrically obtained the position of the rover's COG for various roll angles, and subsequently, we calculated the wheels' loads for various slopes by using (7) and (8). Fig. 8 shows the relationship between the inclination of the slope  $\alpha$ , and the ratio of downhill wheel load to uphill one,  $W_d/W_u$  with different roll angle of the rover,  $\psi_h$ . As observed from the figure, as the slope angle increases, the ratio of wheel loads increases. In addition,  $W_d/W_u$  decreases with increase in the roll angle  $\psi_h$ , and when the roll angle equals the slope angle, i.e., the body of the rover is in the horizontal position on the slope,  $W_d$  equals  $W_u$  ( $W_d/W_u = 1$ ).

2) *Experimental setup*: We used a sandbox (2 [m] in length and 1 [m] in width) as shown in Fig. 9. This sandbox can be jacked up manually to obtain a tilt of approximately

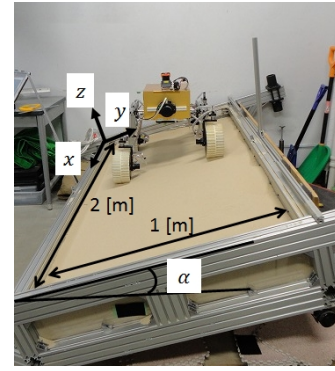


Fig. 9. Test field filled with loose sand

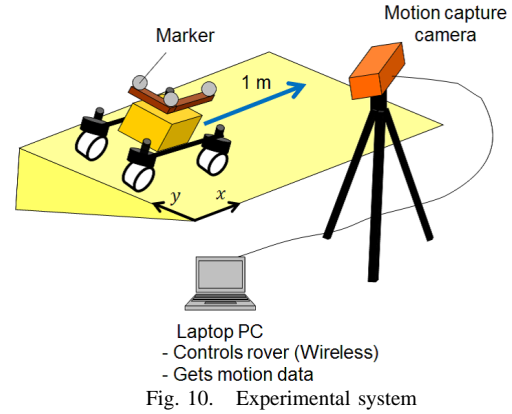


Fig. 10. Experimental system

20 [deg]. The box was uniformly covered with Toyoura standard sand. The mechanical properties of the sand are listed in Table II.

Fig. 10 shows the experimental system. The test bed was operated by a laptop PC via wireless communication. The motion of the rover was tracked using a stereo camera (Stereo Labeling Camera, CyVerse Corp.) with an accuracy of approximately 10 [mm] and a recording frequency of 16 [Hz].

3) *Experimental conditions*: In our traversing experiments, the rover was made to navigate a distance of approximately 1 [m] along the slope in the lateral direction with a velocity of 20 [mm/s]. We varied the roll angle  $\psi_h$  from 0 to 20 [deg] through intervals of 5 [deg], and the inclination angle of the sand box from 10 to 20 [deg] through intervals of 5 [deg]. This experiment was repeated three times under each condition.

4) *Results and discussion*: Fig. 11 shows the measured slip angle for each slope angle. According to this graph, slip angle increases with increasing slope angle values. We

TABLE II  
MECHANICAL PROPERTIES OF TOYOURA STANDARD SAND

| Density<br>$\rho$ [g/cm <sup>3</sup> ] | Particle size<br>[ $\mu$ m] | Cohesion<br>$c$ [kPa] | Internal friction angle<br>$\phi$ [deg] |
|--|-----------------------------|-----------------------|---|
| 1.33 -1.49                             | 106-300                     | 0.0                   | 38.0                                    |

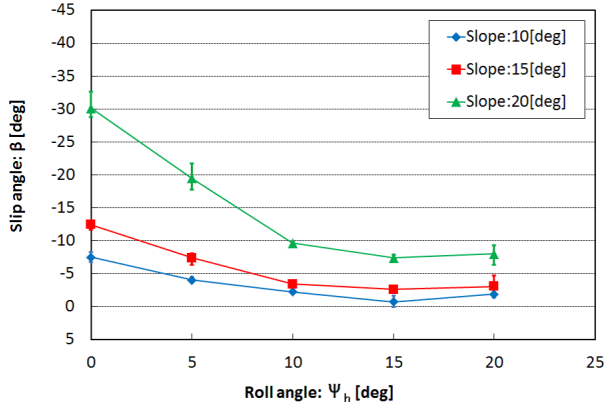


Fig. 11. Results for rover attitude change experiments - roll angle vs. slip angle at various slope angles

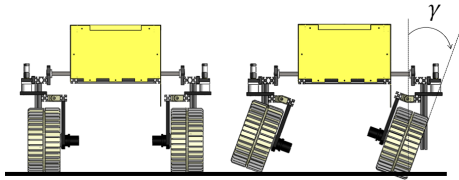


Fig. 12. Rover test bed for wheel angle experiment. Nominal (left) and inclined (right) wheel configuration

speculate that this is because the soil shear margin reduces and this leads to the easier collapse of the slope at increased slope angles, as described in Section II-B. Another possible reason is that the wheel load of the downhill side wheels become larger than those of the uphill wheels, as indicated in Fig. 8.

For a fixed slope angle, the slip angle decreases with increasing roll angle  $\psi_h$ . Moreover, at  $\alpha = 10$  [deg], the slip angle is smaller at  $\psi_h = 15$  [deg] than at  $\psi_h = 10$  [deg]. As observed from the discussion in Section III-A.1, when the rover body becomes horizontal ( $\psi_h = \alpha$ ), sideslip is reduced to a minimum. However, the experimental result indicates that the slip angle reduces when the rover body is tilted at angles greater than this value. This is because the wheel-soil contact angle also changes with the position of the COG. In addition, the graph indicates that even though roll angle is increased, sideslip is not able to be zero. The amount of the residual slippage becomes larger with increasing slope angles.

TABLE III  
SPECIFICATIONS OF THE ROVER TEST BED FOR THE WHEEL ANGLE EXPERIMENT (NOMINAL CONFIGURATION)

|                        |                              |
|------------------------|------------------------------|
| Size [mm]              | L800 × W550 × H400           |
| Mass [kg]              | 24.4                         |
| Wheel size [mm]        | $\phi 200 \times W100$       |
| Tread [mm]             | 440                          |
| Wheel base [mm]        | 600                          |
| Center of gravity [mm] | $L_d = L_u = 220, L_h = 194$ |

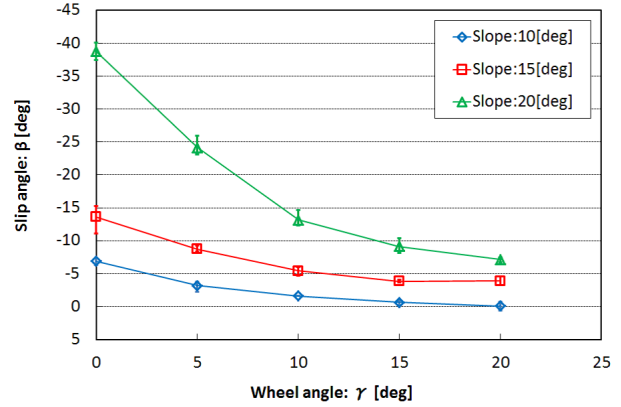


Fig. 13. Results of experiments with wheel angle changes - wheel angle vs. slip angle at various slope angles

### B. Experiments with wheel angle changes

In order to evaluate the effect of the wheel-soil contact angle on downhill sideslip, we conducted slope-traversing experiments under various wheel angles at almost fixed COG values.

1) *Experimental setup*: As illustrated in Fig. 12, we attached extra mechanical parts at the base of the wheels for the experiments with wheel angle changes. By using these parts, the wheel angles can be manually changed while the rover body is parallel to the slopes so that the COG does not largely shift. The rest of the experimental setup was identical to that of the previous experiments with rover attitude changes.

2) *Experimental conditions*: Here, we define the wheel angle,  $\gamma$ , as shown in Fig. 12. For this set of experiments, we varied the wheel angle,  $\gamma$ , from 0 to 20 [deg] through intervals of 5 [deg]. The inclination angle of the sand box was changed from 10 to 20 [deg] through intervals of 5 [deg]. The other conditions were the same as those described in Section III-A.3. The experiments were repeated three times under each condition.

3) *Results and discussion*: Fig. 13 shows the measured slip angle for each value of slope angle,  $\alpha$ , and wheel angle,  $\gamma$ . According to the graph, the slip angle diminishes corresponding to an increase in wheel angle,  $\gamma$ , over all the slopes. However, such the reduction of slippage is limited; this is the same trend as the roll angle experiment.

### C. Evaluation of the effects of attitude change on sideslip

Upon comparing the above two experimental results, we evaluated the effects of shifting the COG and those of changing the wheel-soil contact angle on sideslip. It is noteworthy that the rover's nominal configuration (for example, the tread and the height of the body) in the first and second experiments slightly differed (see Tables I and III). Therefore, we compare both results qualitatively in this section.

From Figs. 11 and 13, it is observed that the changes of slip angle under the variation in the roll angle  $\psi_h$  are in a manner similar to the changes under the variation in the wheel angle  $\gamma$ . In the first experiment, both the COG and

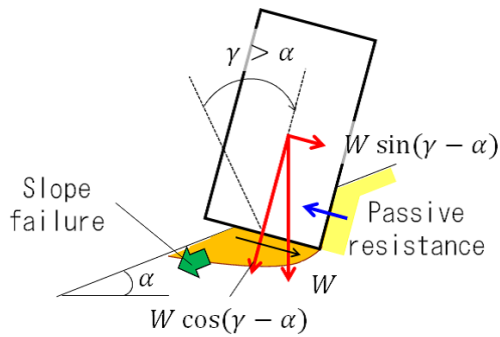


Fig. 14. Slope failure due to the bulldozing effect of wheel's bottom part

wheel-soil contact angle were changed along with the attitude changes. Thus, these results indicate that the effect of shifting COG does not lead to any significant sideslip reduction. That is, the wheel-soil contact angle is an important factor in reducing sideslip.

Next, we discuss as to why modifying the position of the COG did not cause a significant reduction in sideslip. As described in Section II-C.1, the primary advantage in shifting the rover's COG is that the shear stress at the downhill side wheels is reduced. However, if the shear stress largely exceeds the shear margin, regardless of the COG position, the degree of soil failure cannot be further improved even when the wheel loads are reallocated. In particular, on steep slopes, the effect of shifting the COG is insignificant in terms of sideslip reduction because the shear margin reduces, as shown in Fig. 3.

On the other hand, when the wheels are tilted or lean along the uphill direction, the amount of gravitational force along slip direction decreases. Besides, they can interact with the deeper and stronger part of the soil. This leads to reduce probability of slope failure, as described in Section II-C.2. However, as experiments showed, the reduction of the slippage is limited. This is because the gravity force vertical to the sideslip acts in downhill direction when wheel angle,  $\gamma$ , becomes larger than slope angle,  $\alpha$ , as described in Fig. 14. Due to this, soil beneath the wheel is bulldozed downhill along with the wheel rotation and downhill sideslip occurs.

In this light, the tilting of the wheels is effective in reducing the downhill sideslip. However, further investigations are required to quantitatively evaluate the bulldozing effect of the wheel's bottom part on sideslip. By accounting for this factor in the rover modeling, we can obtain the optimal wheel angles or wheel shapes for slope traversing.

#### IV. CONCLUSION AND FUTURE WORK

##### A. Conclusion

In this study, we evaluated the effects of the reconfiguration of exploration rovers that traverse sandy side slopes on downhill sideslip based on the slope failure mechanism and slope-traversing experiments. The experimental results showed that the wheel-soil contact angle is dominant to wheel slippage rather than the rover's COG. This means that it is essential to model forces acting on wheels considering its contact angles against slopes.

##### B. Future work

As regards the future work in this direction, models of bulldozing effect of the wheel's bottom part are required in order to develop wheel-soil contact model on sandy slopes. To achieve this objective, we plan to measure the bulldozing force on slopes and quantitatively evaluate the influence of wheel-soil contact angle on the slopes.

#### REFERENCES

- [1] M. G. Bekker, *Introduction to Terrain-Vehicle Systems*, Ann Arbor, MI, USA, University of Michigan Press, 1969.
- [2] J. Y. Wong, *Theory of Ground Vehicles*, John Wiley & Sons Inc., 1978.
- [3] J. Y. Wong and A. R. Reece, "Prediction of Rigid Wheel Performance Based on the Analysis of Soil-Wheel Stresses," *Journal of Terramechanics*, vol. 4, no. 1, pp.81-98, 1967.
- [4] L. E. Ray, "Estimation of Terrain Forces and Parameters for Rigid-Wheeled Vehicles," *IEEE Transactions on Robotics*, vol. 25, no. 3, pp.717-726, 2009.
- [5] K. Sato, K. Nagatani, and K. Yoshida, "Online Estimation of Climbing Ability for Wheeled Mobile Robots on Loose Soil based on Normal Stress Measurement," *The 19th JAXA Workshop on Astrodynamics and Flight Mechanics*, 2009.
- [6] J. Y. Wong and W. Huang, "Wheels vs. Tracks - A Fundamental Evaluation from the Traction Perspective," *Journal of Terramechanics*, vol. 43, issue 1, pp.27-42, 2006.
- [7] J. P. Pruiksma, J. A. M. Teunissen, G. A. M. Kruse, and M. F. P. Van Winnendael, "Assessment of Tractive Performances of Planetary Rovers with Flexible Wheels Operating in Loosely Packed Soils," *Proceedings of the 10th International Symposium on Artificial Intelligence, Robotics and Automation in Space*, pp.515-522, 2010.
- [8] M. Sutoh, J. Yusa, K. Nagatani, and K. Yoshida, "Traveling Performance Evaluation for Planetary Rovers on Weak Soil," *Proceedings of the 10th International Symposium on Artificial Intelligence, Robotics and Automation in Space*, pp.546-551, 2010.
- [9] D. M. Helmick, S. I. Roumeliotis, Y. Cheng, D. S. Clouse, M. Bajracharya, and L. H. Matthies, "Slip-Compensated Path Following for Planetary Exploration Rovers," *Journal of Advanced Robotics*, vol. 20, no. 11, pp.1257-1280, 2006.
- [10] G. Ishigami, K. Nagatani, and K. Yoshida, "Slope Traversal Controls for Planetary Exploration Rover on Sandy Terrain," *Journal of Field Robotics*, vol. 26, no. 3, pp.264-286, 2009.
- [11] S. V. Sreenivasan, and B. H. Wilcox, "Stability and Traction Control of an Actively Actuated Micro-Rover," *Journal of Robotic Systems*, vol. 11, no. 6, pp.287- 502, 1994.
- [12] K. Iagnemma, A. Rzepniewski, S. Dubowsky, and P. Schenker, "Control of Robotic Vehicles with Actively Articulated Suspensions in Rough Terrain," *Autonomous Robotics*, vol. 14, pp.5-16, 2003.
- [13] C. Grand, F. BenAmar, F. Plumet, P. Bidaud, "Stability and traction optimization of reconfigurable vehicles. Application to an hybrid wheel-legged robot," *The International Journal of Robotics Research*, vol. 23, no. 10-11, pp.1041-1058, 2004.
- [14] G. Freitas, G. Gleizer, F. Lizarralde, and L. Hsu, "Kinematic Reconfigurability Control for an Environmental Mobile Robot Operating in the Amazon Rain Forest," *Journal of Field Robotics*, vol. 27, no. 2, pp.197-216, 2010.
- [15] G. Ishigami, A. Miwa, K. Nagatani, and K. Yoshida, "Terramechanics-based Analysis on Slope Traversability for a Planetary Exploration Rover," *Proceedings of the 25th International Symposium on Space Technology and Science*, pp.1025-1030, 2006.
- [16] D. Wettergreen, S. Moreland, K. Skonieczny, D. Jonak, D. Kohanbash, and J. Teza, "Design and Field Experimentation of a Prototype Lunar Prospector," *The International Journal of Robotics Research*, vol. 29, no. 12, pp.1550-1564, 2010.
- [17] G. Ishigami, A. Miwa, K. Nagatani, and K. Yoshida, "Terramechanics-based Model for Steering Maneuver of Planetary Exploration Rovers on Loose Soil," *Journal of Field Robotics*, vol. 24, no.3, pp.233-250, 2007.
- [18] J. K. Mitchell and K. Soga, *Fundamentals of Soil Behavior*, Third Edition, John Wiley & Sons, Inc., 2005.